



## Growth Mechanism of ZnO Nanostructures Grown by Chemical Method

*Surajit Mandal*

*Department of Physics,*

*Burdwan Raj College, Burdwan, (West Bengal), India*

*(Corresponding author: Surajit Mandal)*

*(Received 19 October, 2017 accepted 18 November, 2017)*

*(Published by Research Trend, Website: [www.researchtrend.net](http://www.researchtrend.net))*

**ABSTRACT:** The growth mechanism of hexagonal shaped ZnO nanorods, grown on Si (100) substrates by hydrothermal method, is investigated. ZnO nanorods were fabricated at an optimized growth temperature of ~ 90°C. X-ray diffraction patterns reveal the formation of wurtzite structure. Structural properties were investigated by field emission scanning electron and transmission electron microscopy. The differential growth rate of above mentioned crystal faces leads to the formation of hexagonal nanorods. The room temperature photoluminescence properties of ZnO nanorods have been studied. In photoluminescence spectra the mechanism of ultraviolet (UV) and green emission of ZnO nanostructure is investigated.

**Key words:** ZnO, nanostructure, photoluminescence, hydrothermal method

### I. INTRODUCTION

Semiconductors with wide band gaps, i.e. corresponding to photon energies in the blue and ultraviolet regimes have great technological interests. Band-gap tuning can be made by forming alloys of the compounds, with band gaps spanning the range of interest and new devices based on superlattices of such compounds has been designed to fill particular requirement of electronic and optical properties. For instance, ZnO has found to be a suitable candidate for device applications; like UV LEDs and UV lasers etc. The optical properties of this material can be tuned chemically by varying the composition and making alloy with other materials. Also, strains developed in the sample strongly affect the band gap and therefore it is also a convenient tool for adjusting the electronic structure of the system [1-3]. Currently, ZnO is a key technological material. It is a very important compound semiconductor with wide band-gap (3.2eV) and large exciton binding energy (~ 60meV) at room temperature [4]. It has been extensively investigated due to its wide technological applications ranging from catalytic, electrical, optoelectronic, photochemistry fields to the room -temperature blue-ultraviolet laser region[4-7]. As a gas sensing material it is very sensitive to many gases (CO, NH<sub>3</sub> etc) with satisfactory stability [8]. As a material for dye-sensitized solar cells, ZnO exhibits an improved performance [9]. In the form of a thin film ZnO is a potential candidate for flat display screen usage [10].

A recent report also reveals that ZnO is also a promising material for using as an electrode in photo-cells. It is also a very suitable material for UV light-emitting diodes and room temperature UV lasers [11, 12]. In, addition ZnO can be made as transparent and highly conductive, or piezoelectric components as well [13]. Therefore, lots of studies with respect synthesis and properties of ZnO nanostructures have been done to meet demands of its potential applications. Till now various physical process related methods such as chemical vapor deposition, thermal evaporation, vapor deposition, thermal decomposition, arc plasma deposition, sputtering, molecular-beam-epitaxy; chemical routes such as hydrothermal and solvothermal, solid state reaction, sol-gel, precipitation, template-based and solution-based processes have been employed to produce ZnO-nanostructures. Well defined nanostructures of ZnO with abundant morphologies such as nanorods, nanobelts, nanotubes as well as other unusual morphologies such as flower, snowflake, prism etc have been developed. These can be realized by simply varying different reaction parameters. It has been observed that optical properties of various typical morphologies show a morphology-dependent features induced by the crystal quality due to morphology variations. Such an abundant morphology world of ZnO provide better understanding of crystal nucleation and growth mechanism from various aspects and would provide possible candidates for nanodevice construction for various applications [7,17].

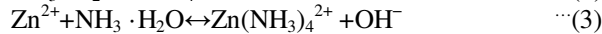
The morphological and structural evolution of hydrothermally deposited ZnO nanostructures on Si substrate using low concentration aqueous solution of Zinc chloride precursor is reported in this paper. Uniform hexagonal shaped nanorods are found to be formed at a certain temperature. The optical property of the nanorods has been investigated by photoluminescence spectroscopy.

## II. EXPERIMENTAL

ZnO nanostructure was fabricated on Si substrates by a hydrothermal decomposition method. The reaction solution was prepared by adding 5 ml ammonia (25%) into a 100 ml zinc chloride solution ( $\text{ZnCl}_2$ , 0.1 M) to maintain the pH value of 9.0. As-prepared solution was poured into a bottle with autoclavable screw cap. The substrate was placed vertically dipped into the reaction solution inside the bottles. The closed bottles were kept on a hot plate to undergo reaction at  $90^\circ\text{C}$  for duration of 1 hour. Subsequently, the bottle was cooled down to room temperature in about 2 hour. The sample was taken out of the bottle as soon as they reach room temperature. On completion of growth, the sample was thoroughly rinsed with the ultrapure water to eliminate residual salts and annealed in oxygen environment at  $300^\circ\text{C}$  for 1 hour. The morphology of the ZnO was examined using a field-emission scanning electron microscope (FE-SEM, ZEISS). The grown nanostructures were characterized by X-ray diffractometer (Philips X-Pert MRD) using  $\text{CuK}_\alpha$  radiation of wavelength  $1.5418\text{ \AA}$  at grazing incidence mode.

## III. RESULTS AND DISCUSSION

The morphologies of the grown nanostructure have been examined using FESEM image. Growth is found to be quite uniform all over the substrate. The oppositely charged ions produce positively charged Zn-(001) and negatively charged O-(001) surfaces, which are atomically flat and stable and without reconstruction [18]. The morphology and structure depend on the time, temperature, and pH of the solution. The dissolution and chemical reactions involved in the formation of ZnO nanostructures are as follows:



During the first stage of the synthesis process, i.e., at a temperature of  $90^\circ\text{C}$ ,  $\text{Zn}(\text{NH}_3)_4^{2+}$  reacts with  $\text{OH}^-$ , to form ZnO nuclei (the equilibrium in the Eq. (4) moves to the right), which deposits on the substrate. Since initially the concentration of  $\text{Zn}(\text{NH}_3)_4^{2+}$  is high, the growth of ZnO nuclei is dominant. Tapered nanorods gradually grow from such nuclei, as shown in Fig. 1. Most of the nanorods are highly oriented and densely populated with homogeneous shape and size. Observed nanorods correspond to the basal plane of the hexagonal crystal structure. The diagonal length of the nanorod is nearly 200 nm with length approximately  $1\text{ }\mu\text{m}$ . The tips of the nanorod are tapered or pyramidal shaped with small surface area (shown in Fig. 1). Tapered or hexagonal pyramidal shaped surfaces are observed on top of the nanorod, as shown in Fig. 1. It is known from the coordination structure of the oxide crystal that the elements of the coordination polyhedron present at different interfaces are different [19, 20]. So the growth rate of various crystal faces is mainly determined by the elements of the coordination polyhedron present at the interface. The face of the nanorods are hexagonal shaped. The growth habit of crystals is due to difference of relative growth rates at various crystal faces. The hexagonal nano-structure with six defined facets arose to maintain the minimum surface energy as to keep the symmetry of the crystal structure (wurtzite ZnO). The velocities of crystal growth is found to be  $V_{\langle 100 \rangle} = V_{\langle 010 \rangle} = V_{\langle 001 \rangle}$ , which is different from maximum crystal growth velocity ( $V_{\langle 001 \rangle}$ ) along c axis [16]. This feature is attributed to the normal growth velocity being greater than the velocity in the lateral direction to the substrate. The growth rate is always greater along the c-axis (in (002) direction) and crystalline orientation is revealed by XRD patterns. Therefore the differential growth rate of above mentioned crystal faces leads to the formation of hexagonal nanorod, as shown in Fig. 1. The XRD pattern of the ZnO nanostructures are shown in Fig. 2, which proves that the nanorods have a wurtzite structure. The entire diffraction peaks match with the well indexed to the hexagonal phase ZnO reported in JCPDS (card No. 36-1451  $a=3.249\text{ \AA}$ ,  $c=5.206\text{ \AA}$ ). From the XRD pattern, it is clear that the tendency of the growth of the nanostructures is in (002) direction i.e. along c-axis though we cannot say that the structure is single crystalline but composed of several crystalline phases. Stoichiometric ZnO is an insulator and contains large voids, which can easily accommodate interstitial atoms. Consequently, it is virtually impossible to prepare pure crystals. It also tends to lose oxygen when heated to a very high temperature [21].

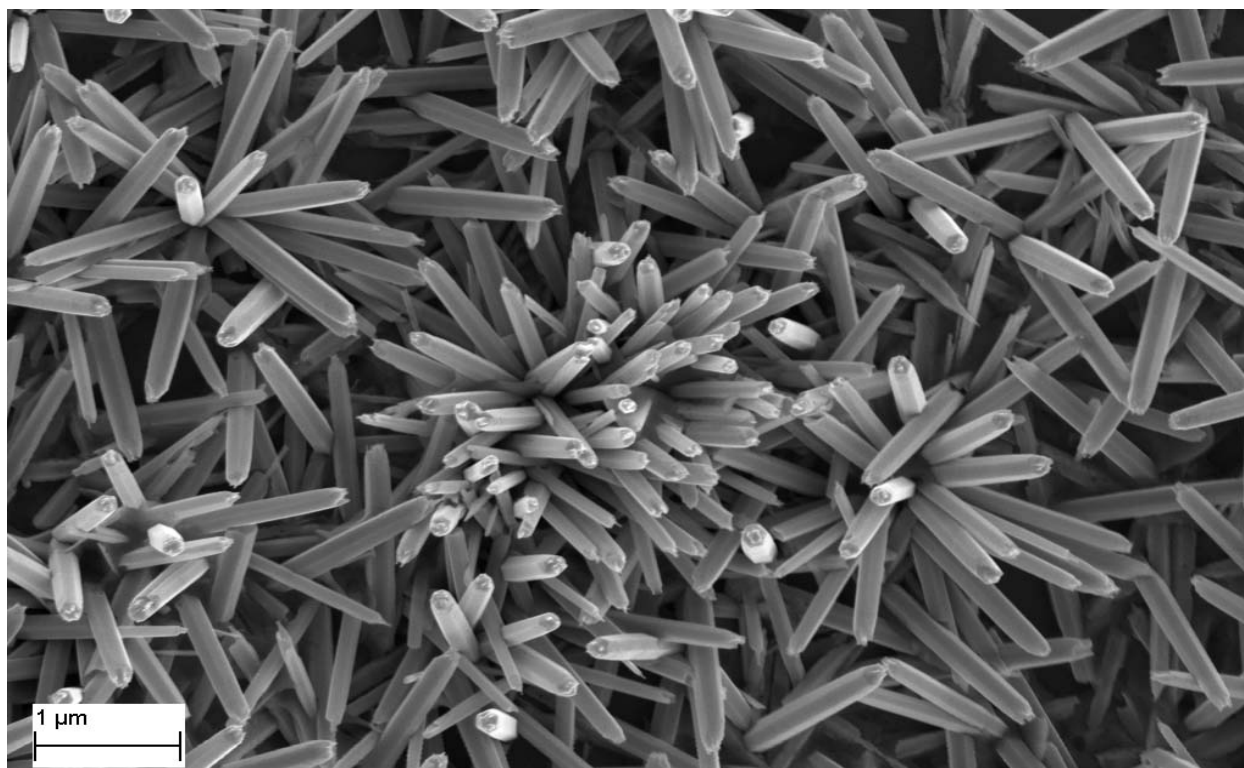


Fig. 1. FE-SEM micrographs of ZnO nanostructures.

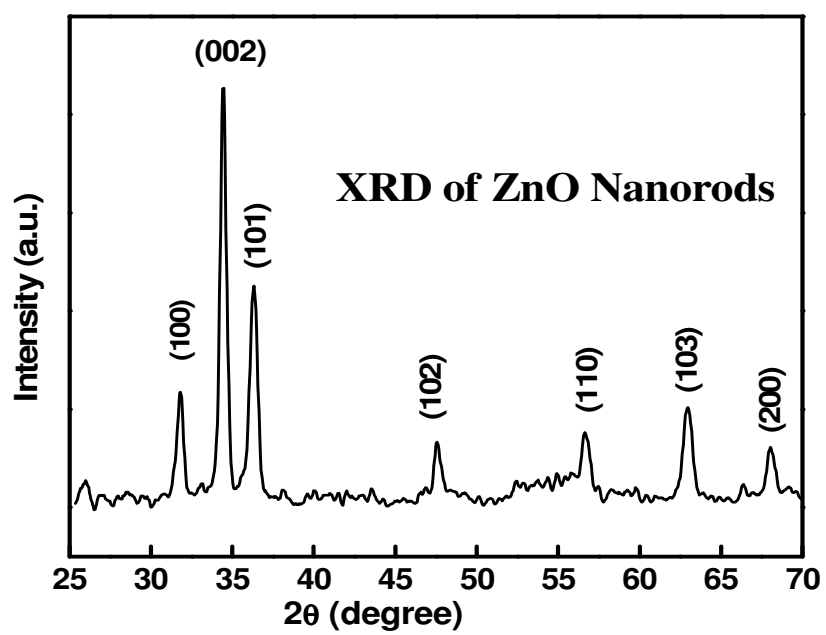


Fig. 2. Grazing incidence XRD pattern of ZnO nanorods.

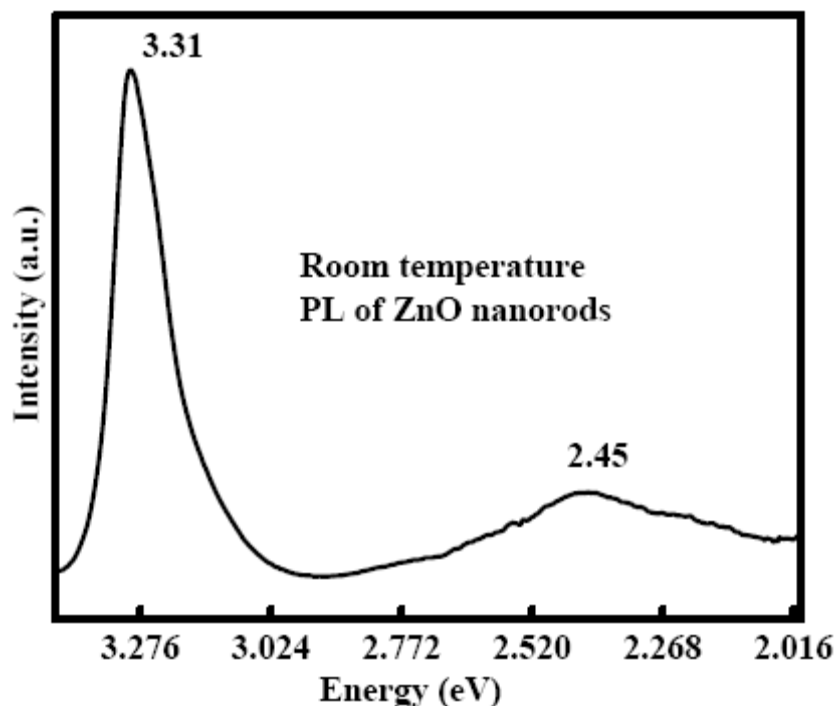


Fig. 3. Room temperature photoluminescence of ZnO nanorods.

For these reasons, ZnO exhibits *n*-type semiconducting properties with inherent defects, such as the lack of O and the excess of Zn. In this regard, the study of the PL characteristics of ZnO is interesting because it can provide valuable information on the quality and purity of the materials. Photoluminescence (PL) is an important property, which provides information on the optically active defects and relaxation pathways of excited states. PL study is useful to identify the origin of sub-band-gap luminescence. Fig. 3 shows the room temperature photoluminescence spectra of ZnO nanostructures. The ultraviolet emission at 3.31 eV of ZnO is attributed to the excitonic one originating from the recombination of free excitons [22], while the origin of blue-green emission at 2.45 eV relates to the oxygen vacancy ( $V_O$ ). The blue-green emission results from the recombination of a photo generated hole with the singly charged oxygen vacancy or zinc interstitial [23].

#### IV. CONCLUSION

ZnO nanostructures of different morphologies were fabricated at a relatively low temperature by a simple hydrothermal method using a mixture of ammonia and zinc chloride solution. The grazing angle XRD revealed the formation of wurtzite structure ZnO. Optical properties of nanorods have been studied in detail using photoluminescence spectroscopy. PL spectra have demonstrated that the emission due to defect energy

states is negligible in comparison with the near band edge emission in the UV-region.

#### ACKNOWLEDGEMENTS

I am grateful to Prof. S. K. Ray (Professor of IIT Kharagpur, Department of Physics and Meteorology) for giving me the opportunity to provide all the Laboratory facilities.

#### REFERENCES

- [1]. C. Ricolleau; L. Audinet; M. Gandais; T. Gacoin and J.P. Boilot; (1999). *Journal of Crystal Growth* **203**: 486-499.
- [2]. J.F. Donegan; (2005). Large Gap II-VI Semiconductors, Semiconductor Materials; Elsevier Ltd.; (2005) 377-385.
- [3]. E. Christensen, I. Gorczyca, O.B. Christtensen, U. Schmid and M Cardona; (1990). *Journal of Crystal Growth*, **101**: 318-331.
- [4]. D.C. Reynolds, D.C. Look, B. Jogai, J.E. Hoelscher, R.E. Sheriff, M.T. Harris, M.J. Callahan; (2000). *J. Appl. Phys.*, **88**, 2152.
- [5]. C.R. Lee, H.W. Lee, J.S. Song, W.Wim, S. Park; (2001). *J. Mater. Synth. Process*; **9**, 281.
- [6]. L. Vayssieres, K. Keis, A. Hagfeldth, S.E. Lindquist; (2001). *Chem. Mater.* **13**, 4386.
- [7]. C.H. Yan, J. Zhang, L.D. Sun; Encyclopedia of Nanoscience and Nanotechnology, edited by H.S. Nalwa; Vol. **10**(767-780).
- [8]. T. Seiyama, A. Kato; (1962). *Anal. Chem.*, **34**, 1502.
- [9]. K. Hara, T. Horiguchi, T. Kinoshita, K. Sayama H. Sugihara, H. Arakawa; (2000). *Sol. Energy Mater. Sol. Cells*; **64** 115.

- [10]. D.S. Ginley, C. Bright; (2000). *Mater. Res. Bull.* **25**, 15.
- [11]. L. Znaidi, G.J.A. A. Solerllia, S. Benyahia, C. Sanchez, A.V. Kanaev; (2003). *Thin Solid Films*, **428**: 257-262.
- [12]. A. Mitra, R.K. Thareja, V. Ganesan, A. Gupta, P.K. Sahoo, V.N. Kulkarni; (2001). *Applied Surface Science*, **174**: 232-239.
- [13]. M. Hiramatsu, K. Imaeda, N. Horio, M. Nawata; (1998). *J. Vac. Sci. Technol. A* **16**, 669 (1998).
- [14]. Z.L. Wang; (2004). *J. Phys: Condens. Matter* **16**: R829-R858.
- [15]. Mandal S, Dhar A & S. K. Ray, (2009). *J. Appl. Phys.*, **105**: 033513.
- [16]. Mandal S, Sambasivarao K, Dhar A & S. K. Ray, (2009). *J. Appl. Phys.*, **106**: 024103.
- [17]. Mandal S, Mullick H, Dhar A & S. K. Ray, (2008). *J. Electrochem. Soc.*, **155**: K129.
- [18]. Meyer B & Marx D, (2003). *Phys. Rev. B*, **67**: 035403.
- [19]. Li W J, Shi E W, Zhong W Z & Yin Z W, (1999). *J. Cryst. Growth* **203**: 186.
- [20]. Wang R C, Liu C P, Huang J L, Chen S J, Tseng Y K & Kung S C, (2005). *Appl. Phys. Lett.* **87**: 013110.
- [21]. Kwok W M, Djuršić A B, Leung Y H, Chan W K, Philips DL, (2005). *Appl. Phys. Lett.*, **87**: 22311.
- [22]. Fonoberov V A, Alim K A, Balandin A A, Xiu F & J. Liu, (2006). *Phys. Rev. B*, **73**: 165317.
- [23]. Mandal S, Goswami M L N, Das K, Dhar A & Ray S K, (2008). *Thin Solid Films*, **516**: 8702.